

STUDY OF FLOW AROUND NACA0020 AEROFOIL WITH HAIRY FLAPS DURING RAMP-UP MOTION

M. E. Rosti, M. Omidyeganeh, A. Pinelli

Department of Mechanical and Aeronautical Engineering, City University London, EC1V 0HB, London, UK

INTRODUCTION

The challenge of controlling flow separation on the suction side of wings at high angle of attack is the focus of many research activities. Among various designs and ideas, in the last decade biomimetic approaches, especially focusing on emulating the flying modalities of birds, have caught the attention of several researchers. In particular, the self-adaptive characteristics of the wings feathers have inspired passive control methodologies to delay and/or to palliate flow separation in critical flight conditions[2]. One of the observed features on the flight of certain types of birds is the feathers pop up induced by back-flow from the trailing edge towards the leading edge, which occurs when flow separates. It is reported that this mechanism counteract the back-flow, thus avoiding sudden drops in the lift force (e.g., stall condition) [1].

The self-adjusting reaction of feathers to incipient flow separation has inspired the design of hairy flaps located on the suction side of the aerofoils to mitigate the adverse effects of separation (i.e., enhanced lift) [6, 1]. Simple span-wise flaps distributed close to the trailing edge have shown to improve the lift by 10% at a chord Reynolds number of about one million [6]. A simple but appropriate study of stall performance of a given design is the ramp-up motion in which the angle of attack is increased from 0° to some angle after stall $\simeq 20^\circ$. Brücker and Weinder [1] studied the span of the time in which it takes during the ramp-up motion for an aerofoil to stall; the authors show that the onset of stall could be delayed by a factor of 2 to 4 using a particular flaps configuration. The latter features 2 or 3 rows of flaps with the flap sizes and spacings in the order of the thickness of the separation bubble. They also observed interesting modulation of the wake in presence of flaps which may relate to the improvement of the aerodynamic performance in a stalled configuration. When the flaps pop up as a result of the interaction with the separating bubble, they interfere with instability of separated shear layer and inhibit merging of rollers which is believed to be a reason for stall. The separated rollers are shed downstream with a particular frequency despite the turbulent nature of the shear layer in the absence of flaps.

Although a number of experimental measurements have put forward the potential for self adjusting hairy flaps in controlling separation bubbles in stalled and pre-stalled aerofoils conditions, to our knowledge no high fidelity numerical simulations have been carried out so far. Those simulations would pave the way towards a more detailed understanding of the physical mechanisms that determine their interaction with the separated flow field thus enabling the design of more ef-

ficient configurations. In this work, we aim to simulate for the very first time three-dimensional turbulent flow around an NACA0020 aerofoil with hairy flaps installed on the suction side and close to the trailing edge during a ramp-up motion. Through the analysis of the accumulated simulation data we will also shed some light onto the fluid interaction mechanisms that may introduce beneficial effects on the control of the separated regions.

PROBLEM FORMULATION

We assume an incompressible, 3D unsteady flow field, governed by the Navier Stokes equations

$$\frac{\partial u_i}{\partial t} + \frac{\partial u_i u_j}{\partial x_j} = -\frac{\partial P}{\partial x_i} + \frac{1}{Re_\infty} \nabla^2 u_i + f_i, \quad \nabla \cdot \vec{u} = 0 \quad (1)$$

where $Re_\infty = U_\infty c / \nu$, c is the chord length of aerofoil, and U_∞ is the approaching velocity magnitude. $x(u)$, $y(v)$ and $z(w)$ are the chord-wise, vertical and span-wise directions (velocity components). The governing differential equations (1) are discretised on a non-staggered grid using a curvilinear second order centered finite-volume code. A second-order-accurate semi-implicit fractional-step procedure is used for the temporal discretisation (Crank-Nicolson scheme is used for the vertical diffusive terms, and the Adams-Bashforth scheme for all the other terms). The pressure equation that enforces the solenoidal condition on the velocity field is solved via a Fast Poisson Solver that incorporates corrections for grid non-orthogonality. Further details on the code, its paralelisation and the extensive validation campaign can be found in [4].

Figure 1 shows a scheme of NACA0020 aerofoil with the flexible flaps attached in the trailing edge region; d_f is the flaps width, l_f is their length, and s_f is the spacing between them. The flap motion takes place in xy plane (no torsion allowed around their main axis). Each flap is modeled as a lumped 1D flexible filament

$$\Delta \rho \frac{\partial^2 x_i}{\partial t^2} = \frac{\partial}{\partial s} \left(T \frac{\partial x_i}{\partial s} \right) - K_B \frac{\partial^4 x_i}{\partial s^4} - \rho_f a_f \epsilon, \quad (2)$$

where $x_i, i = 1, 2$ are the Cartesian displacements (in x and y), s is the flap parametric coordinate along its length, T is the tension of flap, K_B is the stiffness of flap, ρ_f is density of fluid, a_f is acceleration of fluid at the position of flap integrated along the span for each s coordinate, ϵ is the characteristics hydraulic thickness of the flap (approximately equal to the local fluid grid spacing). $\Delta \rho = \hat{\rho}_s - \hat{\rho}_f$ is the difference in density per unit area of filament cross section between solid flap and fluid. The flap dynamic equation (2) is advanced in

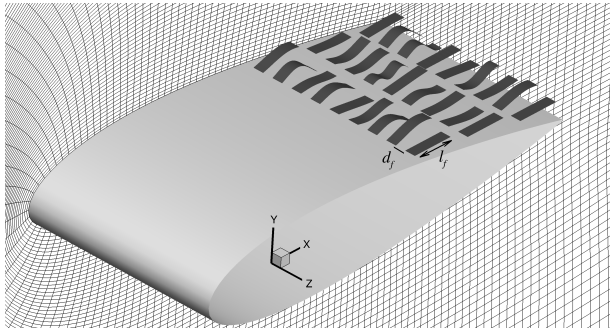


Figure 1: Schematic of NACA0020 aerofoil with flaps attached on the suction side close to trailing edge. Mesh shown on a xy plane (quasi orthogonal grid: $3170 \times 765 \times 96$ points) is skipped every 10 points in both directions. Each flap discretised using 42 equidistributed nodes.

time (under the constraint of inextensibility: $(x_i \ x_i)^{1/2} = 1$) by solving the algebraic non-linear system (arising after a finite difference approximation of the flap equation) via a Newton Raphson method at each time step (see[3] for details on the whole methodology).

Before considering the full geometry incorporating the flexible flaps in a ramp up maneuver, we have validated the code by considering Direct Numerical Simulations (DNS) of the flow around a NACA0020 aerofoil. In particular, we have considered three different angles of attack (that will be swapped in the ramp up motion): 0° , 10° , and 17.5° , at $Re_\infty = 77500$. The mesh adopted for the three incidence angles has been kept the same (the angle of attack is changed by changing the in-flow direction, i.e., the boundary conditions) to verify that the mesh can resolve the shear layers developing in a fully separated condition (see figure 1 for details). At 17.5° we have validated our simulation against experiments by Brücker [1]. The ramp-up motion is modeled by slow increase of the angle of attack from 0° to 17.5° in a span of $5c/U_\infty$. The validation campaign will be continued by employing flaps close to the trailing edge as in Figure 1 with similar parameters in the experiment [1]. The width of all flaps are $d_f = 0.025c$; their spacing in z is equal to their width $s_f = d_f$; their length is $l_f = 0.1c$ and spacing between each row is $0.15c$.

RESULTS AND DISCUSSIONS

Preliminary results in Figure 2 illustrates coherent vorticity structures (defined with the Q-criterion) at an instant of time at three different angles of attack, 0° , 10° , and 17.5° respectively for a smooth wing. The flow at 0° angle of attack is attached to the wing, and the wake is composed by spanwise rollers generated at the trailing edge of the wing. An increase of the angle of attack at 10° exhibits an early flow separation, and the turbulent structure generated over the wing, will eventually interact with the trailing edge vortices to form the wake. In the last picture, at high angle of attack 17.5° , the flow separates in the proximity of the leading edge.

The separation zones are more clearly evident from Figure 3, where the isosurfaces of the zero stream-wise velocity magnitude are shown. At 0° small recirculation zones are present near the trailing edge of the wing on both sides. Increasing the angle of attack at 10° the separation point $x \approx 0.25c$ on the suction side of the wing moves toward the leading edge, while at 17.5° the separation occurs at $x \approx 0.1c$.

Our analysis of the flow around the aerofoil during the ramp-up motion is still on going. Transient response of the

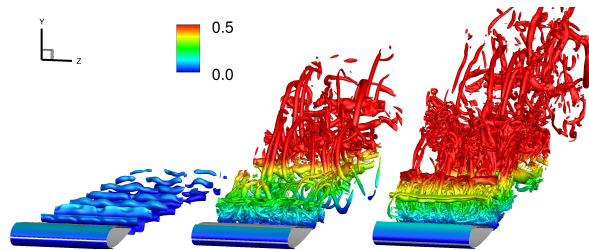


Figure 2: Isosurfaces of Q colored by y/c at 0° , 10° , and 17.5° angles of attack from left to right.

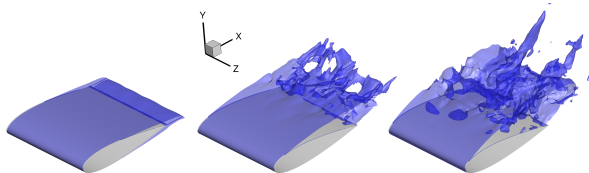


Figure 3: Separated zone represented with the isosurface of stream-wise velocity equal to zero at 0° , 10° , and 17.5° angles of attack from left to right.

mean and instantaneous flow characteristics to time-variant approaching flow is actually been undertaken and the results will be presented at the Meeting. Working in parallel we have also started the simulation campaign of the same wing with above described hairy flaps (see Figure 1) configuration. An analysis on their effects on the detached flow during the ramp-up motion will also be presented.

REFERENCES

- [1] Christoph Brücker and Christoph Weidner. Influence of self-adaptive hairy flaps on the stall delay of an airfoil in ramp-up motion. *Journal of Fluids and Structures*, 47:31–40, 2014.
- [2] Anna C Carruthers, Adrian LR Thomas, and Graham K Taylor. Automatic aeroelastic devices in the wings of a steppe eagle aquila nipalensis. *Journal of Experimental Biology*, 210(23):4136–4149, 2007.
- [3] J. Favier, A. Revell, and A. Pinelli. A lattice boltzmann immersed boundary method to simulate the fluid interaction with moving and slender flexible objects. *J. Comput. Phys.*, 261:145–161, 2014.
- [4] M. Omidyeganeh and U. Piomelli. Large-eddy simulation of two-dimensional dunes in a steady, unidirectional flow. *J. Turbul.*, 12(42):1–31, 2011.
- [5] A. Pinelli, I.Z. Naqavi, U. Piomelli, and J. Favier. Immersed-boundary methods for general finite-difference and finite-volume Navier-Stokes solvers. *J. Comput. Phys.*, 229:9073–9091, 2010.
- [6] Markus Schatz, Thilo Knacke, Frank Thiele, Robert Meyer, Wolfram Hage, and DW Bechert. Separation control by self-activated movable flaps. *AIAA Paper*, 1243:2004, 2004.